

Supporting Information

for

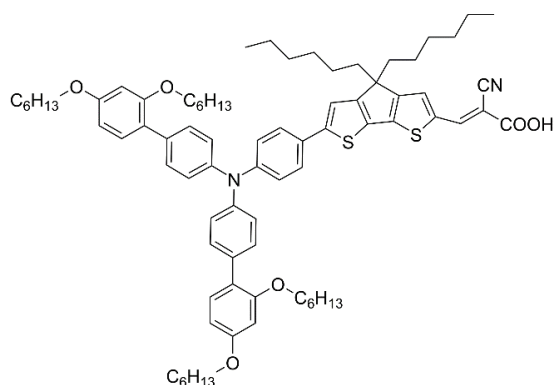
Complexity of Electron Injection Dynamics and Light Soaking Effects in Efficient Dyes for Modern DSSC

Adam Glinka^{1*}, Jacek Kubicki¹ and Marcin Ziólek^{1*}

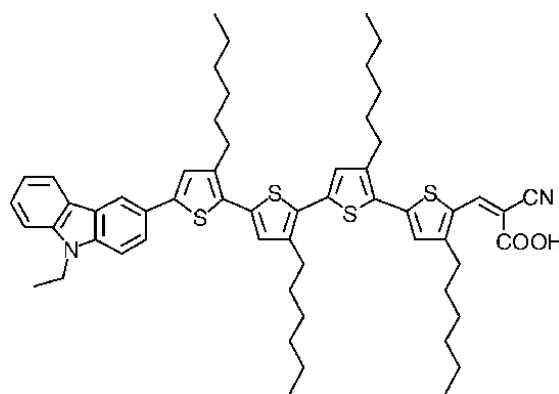
¹ *Quantum Electronics Laboratory, Faculty of Physics, Adam Mickiewicz University in Poznań, Uniwersytetu Poznańskiego 2, 61-614 Poznań, Poland.*

* corresponding authors, emails: adam.glinka@amu.edu.pl (AG) and marziol@amu.edu.pl (MZ)

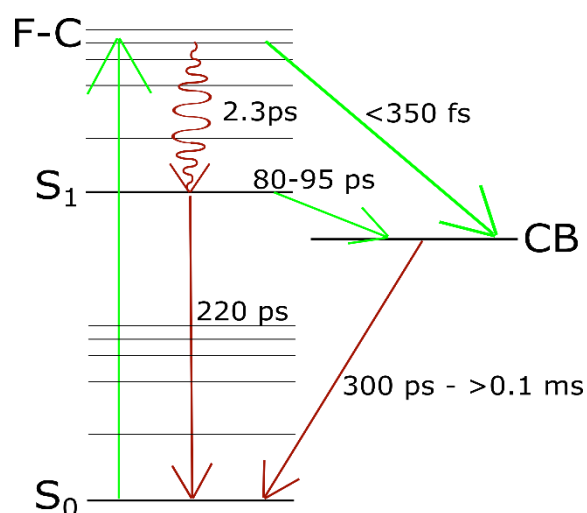
A



B



Scheme S1. Molecular structures of Y123 (A) and MK2 (B)



Scheme S2. Kinetic model of the electron injection from dye to the conduction band of titania in the cells comprising Y123 dye. Green and wine red arrows represent desired and undesired processes, respectively. The vibrational relaxation ($F-C \rightarrow$ relaxed S_1) and internal conversion ($S_1 \rightarrow S_0$) time constants are given based on our TA measurements of Y123 in solution. However, it should be noted that the internal conversion of Y123 attached to nanoparticles was reported to be equal to 750 ps while measured at mesoporous Al_2O_3 substrate [1]. Therefore, the quantum yield of electron injection from Y123 should be close to 100 % from both hot and relaxed excited state.

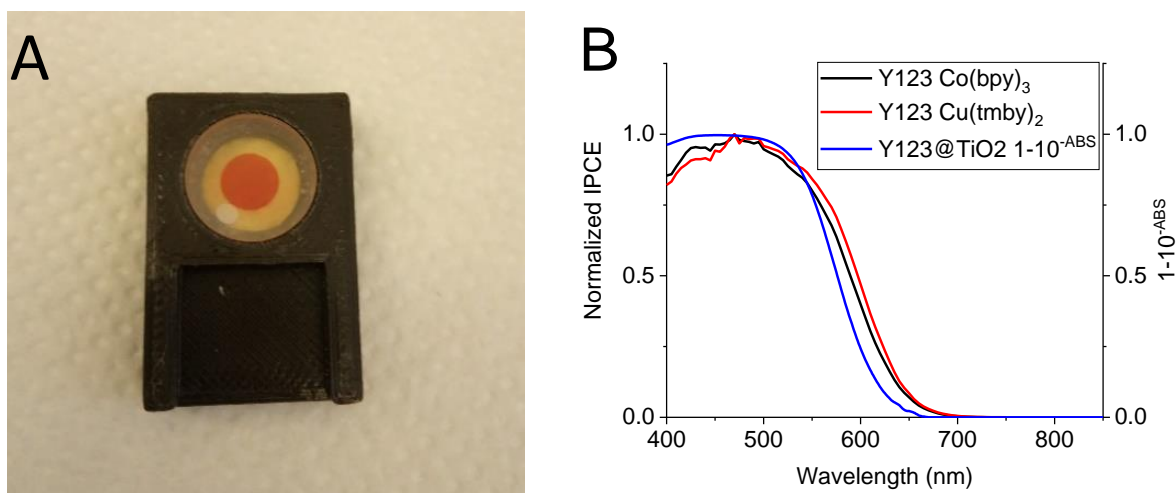


Figure S1. (A) Photo of the half-cell comprising titania sensitized with Y123 dye and cobalt-based electrolyte. The windows are 3mm thick sapphire plates provided by Thorlabs. (B) Normalized IPCE spectra of solar cells containing Y123 in combination with Co- and Cu-based electrolyte in comparison with the dye's absorbance spectra.

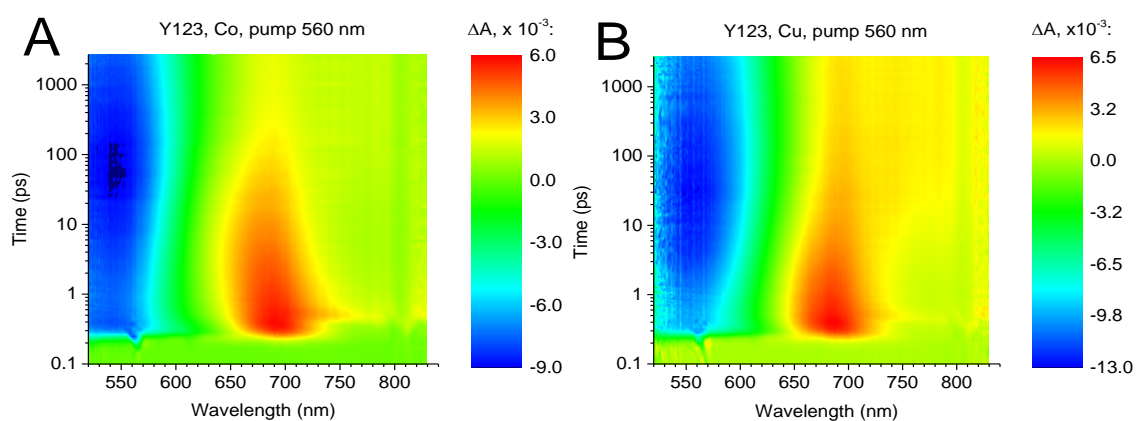


Figure S2. Pseudo-color 2D spectra of original transient absorption data for DSSCs with Y123 dye and (A) cobalt- and (B) copper- based electrolyte. The time zero was shifted to 0.3 ps in order to present the time axis in logarithmic scale.

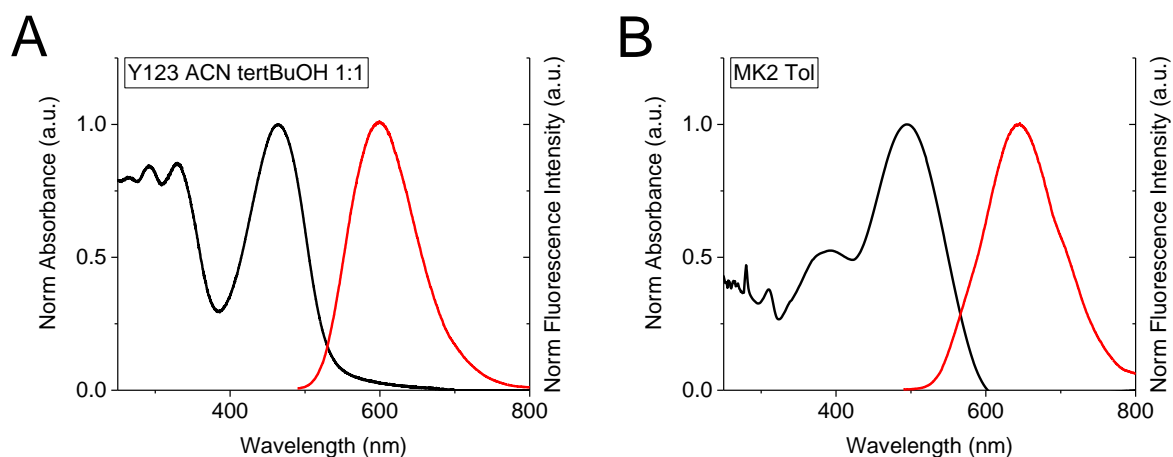


Figure S3. Normalized absorption and fluorescence spectra of the solutions used for sensitization by Y123 dye (A) and MK2 dye (B).

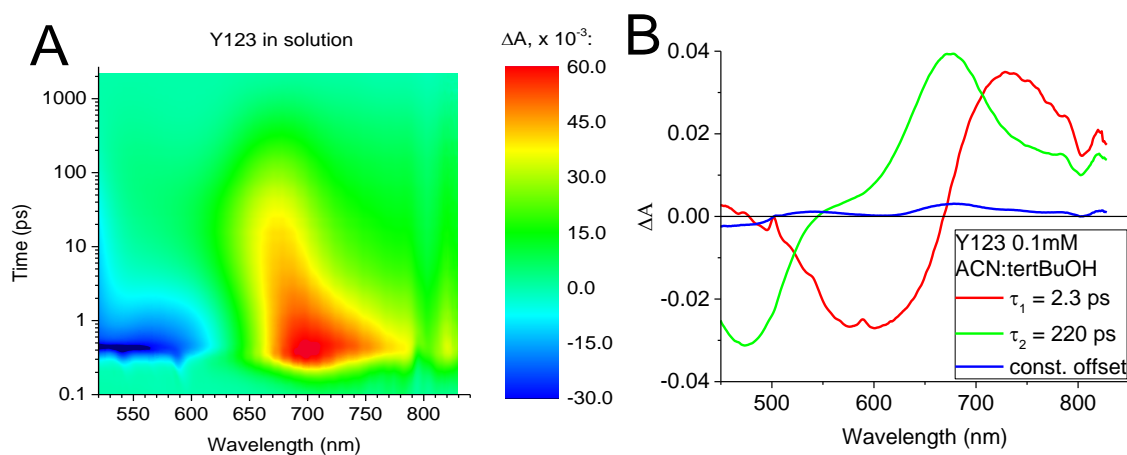


Figure S4. Pseudo-color 2D spectra of original data. The time zero was shifted to 0.3 ps in order to present the time axis in logarithmic scale (A), and global analysis of transient absorption spectra (B) of Y123 in ACN:tert-BuOH solution. The fastest component of about 2 ps should be assigned to the relaxation and solvation process in S_1 state. The shape of its amplitude spectra (negative values below 650 nm and positive above 650 nm) indicate the red shift of transient absorption spectra. The second component of 220 ps represents the decay of the relaxed S_1 state. The small residual component might be due to the triplet state populated with low quantum yield.

Table S1. Time constants obtained in the global analysis of the transient absorption of the solar cells sensitized with Y123 dye and collected for different pump wavelengths.

Co fresh				Cu fresh		
Wavelength [nm]	τ_1 [ps]	τ_2 [ps]	τ_3 [ps]	τ_1 [ps]	τ_2 [ps]	τ_3 [ps]
480	1.7	23	480	1	11	490
560	1	18	370	1.5	12	530
640	1.3	17	400	2	20	380

Co irradi				Cu irradi		
Wavelength [nm]	τ_1 [ps]	τ_2 [ps]	τ_3 [ps]	τ_1 [ps]	τ_2 [ps]	τ_3 [ps]
480	0.6	14	340	0.4	8.3	620
560	0.7	13	310	1.4	10	420
640	1.5	15	360	2.7	28	610

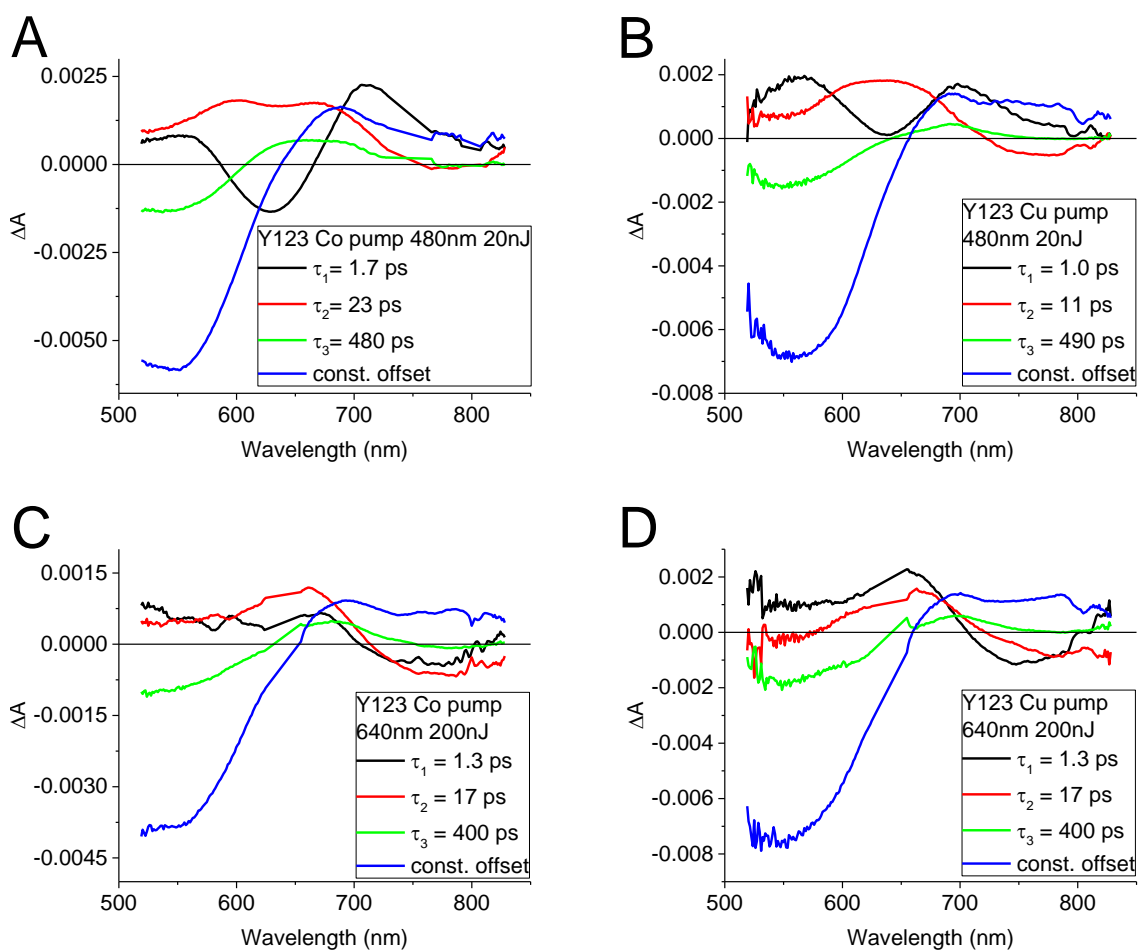


Figure S5. Pre-exponential factor spectra associated to the indicated time constants for a model with a three-exponential function with an offset for DSSC with Y123 dye and cobalt- (A,C) and copper- (B,D) based electrolyte, collected for 480 nm (A,B) and 640 nm (C,D). The fitted time constants for three pump wavelengths are compared in Table S1.

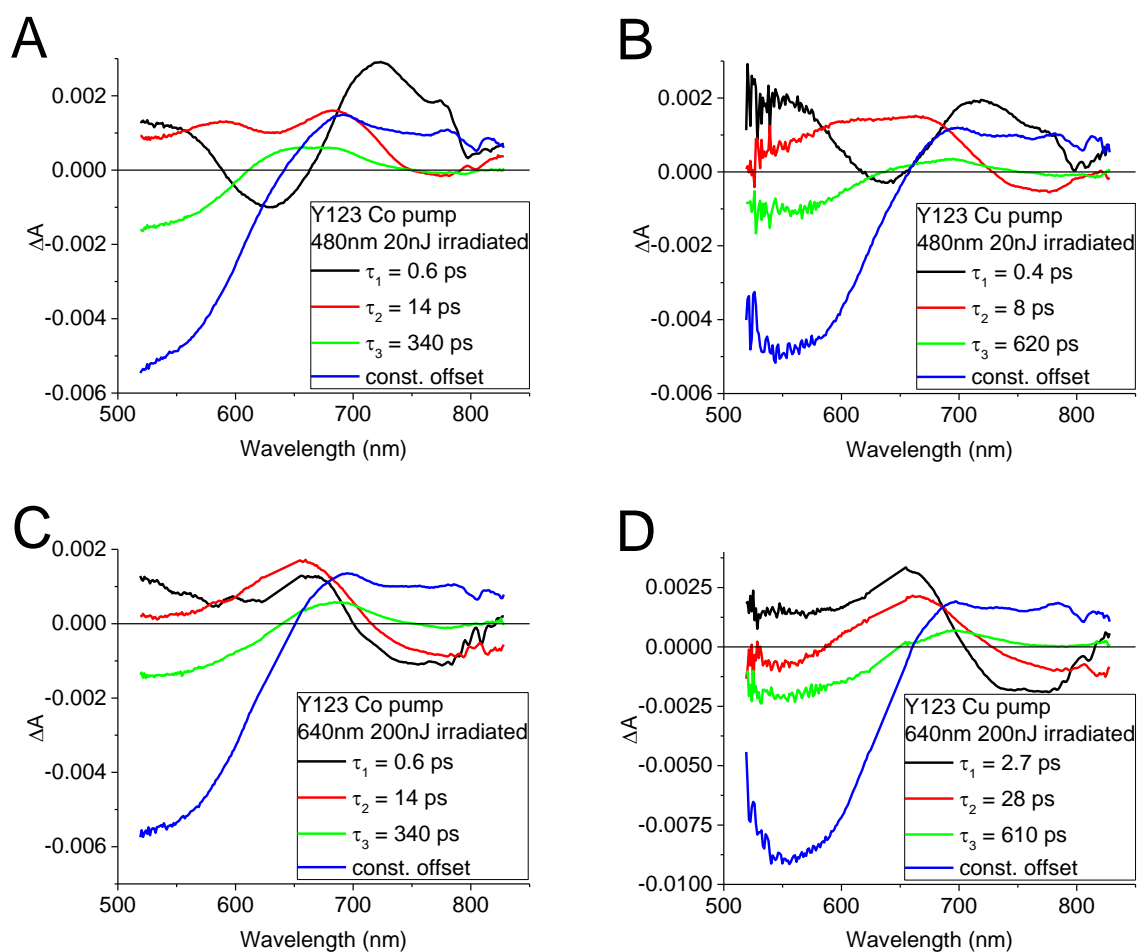


Figure S6. Pre-exponential factor spectra associated to the indicated time constants for a model with a three-exponential function with an offset for irradiated DSSC with Y123 dye and cobalt- (A,C) and copper- (B,D) based electrolyte, collected for 480 nm (A,B) and 640 nm (C,D).

Table S2. Time constants of the poly-exponential functions fitted to the transient absorption kinetics measured at 4780nm wavelength (Figure 3)

Pump pulse energy	Injection fast component	Injection slow component	Contribution of the slower component to the final signal	Recombination component
500 nJ	350 ± 10 fs	93 ± 1 ps	25%	820 ± 10 fs
100 nJ	350 ± 10 fs	85 ± 1 ps	60%	-
50 nJ	350 ± 10 fs	79 ± 1 ps	70%	-

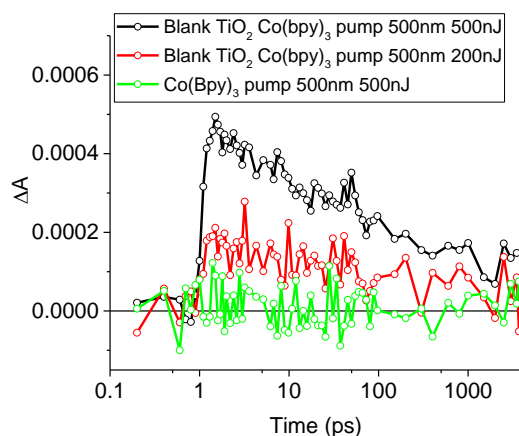


Figure S7. Kinetics of transient absorption at 4780nm collected to exclude the contribution of artifacts from pure TiO₂ and electrolyte to the injection kinetics. The time zero was shifted to 1 ps in order to present the time axis in logarithmic scale.

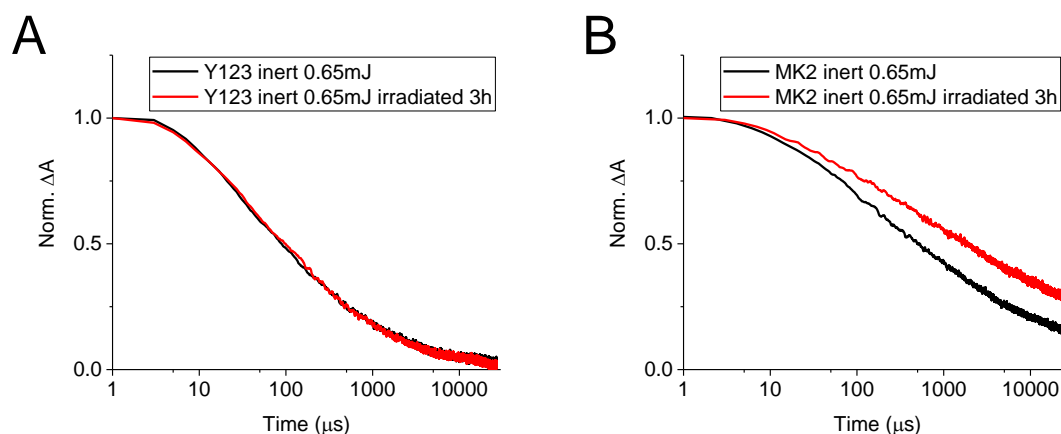


Figure S8. Transient absorption kinetics of the cells containing Y123 (A) and MK2 (B) dyes and inert electrolyte (solution without the addition of redox couple) measured at 700 nm. Transient absorption kinetics in ns-ms timescale were recorded on a nanosecond flash photolysis setup based on a Q-switched Nd:YAG laser as a pump and a 150 W Xe arc lamp as a probe. The pump pulses were set to 532 nm wavelength with 0.65 mJ energy. The probe spectrum was confined using a 10 nm at full width at half maximum (FWHM) band pass interference filter to limit the influence of high intensity probe light on the measured kinetics. The signal was detected by a photomultiplier (R928 Hamamatsu) coupled to a digital oscilloscope (Tektronix TDS 680 C).

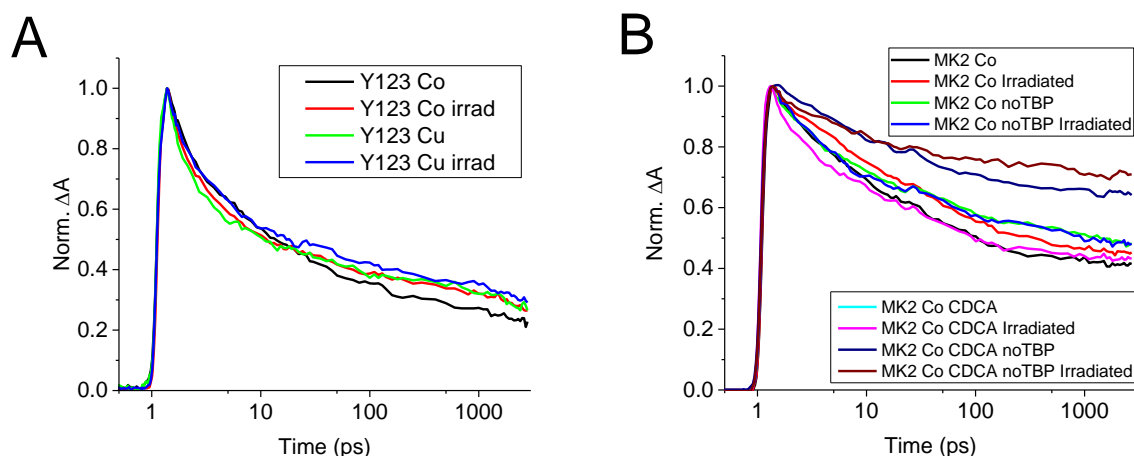


Figure S9. Kinetics of transient absorption of Y123 sensitized cells at 700 nm (A) and MK2 sensitized solar cells at 750nm (B). The time zero was shifted to 1 ps in order to present the time axis in logarithmic scale.

Solar cells with MK2 dye and copper-based electrolyte

Solar cells comprising MK2 dye and $\text{Cu}^{2+/+}(\text{tmby})_2$ exhibited relatively low PCE due to modest J_{SC} and V_{OC} (the latter quite low for copper-based electrolyte). One of the possible reasons for low J_{SC} could be insufficient driving force for dye regeneration. The redox potential of $\text{Cu}^{2+/+}(\text{tmby})_2$ redox couple is equal to -0.87 V vs SHE [2], what gives only 0.08 V over -0.95 V vs SHE for MK2 [3]. Therefore we measured the kinetics of the transient absorption at 700 nm representing the decay of oxidized dye caused by desired reduction reaction involving Cu^+ species (Figure S10A). The time constant of the decay was equal to 7.8 μs . This means that the regeneration process occurs approximately twice slower than 4 μs for MK2 with $\text{Co}^{3+/2+}(\text{bpy})_3$ measured in comparable experimental conditions [4]. However it should be still fast enough taking into account that the kinetics of the competing recombination process (black curve in Figure S10A) is orders of magnitude slower.

The difference in PCE should be rather attributed to low in comparison with Y123 electron lifetime (Figure S10B) explaining both low J_{SC} and V_{OC} values and indicating severe electron recombination from titania to the oxidized form of the redox mediator in the absence of bulky blocking dye moieties in MK2 dye [5].

Table S3. Photovoltaic parameters of the cells comprising MK2 and copper-based electrolyte ^a

	PCE [%]	Voc [V]	FF	Jsc [mA cm ⁻²]	Total APCE
MK2 Cu^{2+/+}(tmby)₂	2.2	0.82	0.76	3.50	0.37
error	0.1	0.01	0.01	0.17	0.02

^a PCE, power conversion efficiency; V_{OC}, open circuit voltage; J_{SC}, short circuit photocurrent density; FF, fill factor. Parameters were averaged from at least three devices. Errors were calculated as the standard deviation of the mean value.

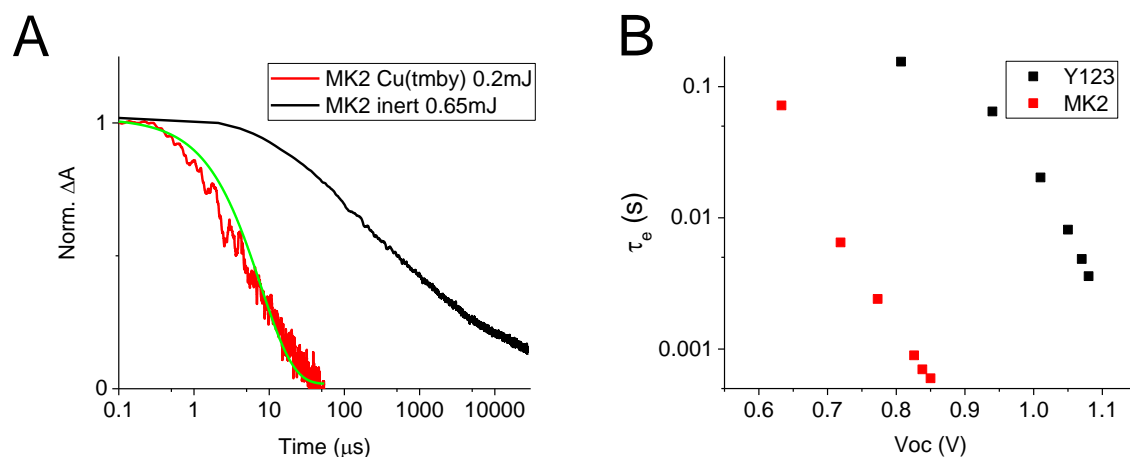


Figure S10. Transient absorption kinetics of the cells containing MK2 dye and copper-based and inert electrolyte (solution without the addition of redox couple) measured at 700 nm. Pump wavelength was set to 532 nm. Time constant of the fitted curve was equal to $7.8 \pm 0.1 \mu\text{s}$ (A), small light perturbation electron lifetime measurements of the cells comprising Y123 and MK2 dyes in combination with Cu^{2+/+}(tmby)₂ redox couple (B). Electron lifetimes were obtained using a Dyenamo Toolbox setup. Measurements were performed in open circuit conditions. A square wave modulated white light illumination was applied and the photovoltage response was acquired and analyzed by a dedicated software using the first order kinetics model.

The effect of light soaking is very pronounced and beneficial for cells comprising MK2 and Cu^{2+/+}(tmby)₂ (Table S4: 25% rise of photocurrent density, beneficial FF change and finally over 30% PCE enhancement).

Table S4. The ratios of photovoltaic parameters measured after and before 30 min continuous irradiation of the cells comprising MK2 and copper-based electrolyte

	PCE ratio	Voc ratio	FF ratio	Jsc ratio
MK2 Cu^{2+/+}(tmby)₂	1.31	1.00	1.06	1.25

Taking into account the magnitude of this light soaking effect and severe titania-electrolyte recombination as the bottleneck in hereby discussed system, it seems reasonable to

suspect that the boost of the photovoltaic performance could be attributed (except the factors discussed in the main part of this work) to the slowdown of the titania-electrolyte recombination dynamics. This could be related with the advantageous modifications in coordination spheres of the Cu²⁺ complexes with participation of the TBP [6–9] associated with the alterations in Li⁺ and H⁺ and the Lewis base equilibrium on the titania/dye/electrolyte interface mentioned in the main part of the work. However, despite being tempting, elucidation of this phenomena exceeds the scope of this work.

References

1. Cao, Y.; Saygili, Y.; Ummadisingu, A.; Teuscher, J.; Luo, J.; Pellet, N.; Giordano, F.; Zakeeruddin, S.M.; Moser, J.-E.; Freitag, M.; et al. 11% efficiency solid-state dye-sensitized solar cells with copper(II/I) hole transport materials. *Nat. Commun.* **2017**, *8*, 15390.
2. Saygili, Y.; Söderberg, M.; Pellet, N.; Giordano, F.; Cao, Y.; Munoz-García, A.B.; Zakeeruddin, S.M.; Vlachopoulos, N.; Pavone, M.; Boschloo, G.; et al. Copper Bipyridyl Redox Mediators for Dye-Sensitized Solar Cells with High Photovoltage. *J. Am. Chem. Soc.* **2016**, *138*, 15087–15096.
3. Kakiage, K.; Aoyama, Y.; Yano, T.; Otsuka, T.; Kyomen, T.; Unno, M.; Hanaya, M. An achievement of over 12 percent efficiency in an organic dye-sensitized solar cell. *Chem. Commun.* **2014**, *50*, 6379–6381.
4. Sobuś, J.; Gierczyk, B.; Burdziński, G.; Jancelewicz, M.; Polanski, E.; Hagfeldt, A.; Ziótek, M. Factors Affecting the Performance of Champion Silyl-Anchor Carbazole Dye Revealed in the Femtosecond to Second Studies of Complete ADEKA-1 Sensitized Solar Cells. *Chem. - A Eur. J.* **2016**, *22*, 15807–15818.
5. Glinka, A.; Gierszewski, M.; Gierczyk, B.; Burdziński, G.; Michaels, H.; Freitag, M.; Ziótek, M. Interface Modification and Exceptionally Fast Regeneration in Copper Mediated Solar Cells Sensitized with Indoline Dyes. *J. Phys. Chem. C* **2020**, *124*, 2895–2906.
6. Saygili, Y.; Stojanovic, M.; Michaels, H.; Tjepelt, J.; Teuscher, J.; Massaro, A.; Pavone, M.; Giordano, F.; Zakeeruddin, S.M.; Boschloo, G.; et al. Effect of Coordination Sphere Geometry of Copper Redox Mediators on Regeneration and Recombination Behavior in Dye-Sensitized Solar Cell Applications. *ACS Appl. Energy Mater* **2018**, *1*, 4950–4962.
7. Ho, W.L.; Katz, M.J.; Deria, P.; Iii, G.E.C.; Pellin, M.J.; Farha, O.K.; Hupp, J.T. One Electron Changes Everything. A Multispecies Copper Redox Shuttle for Dye-Sensitized Solar Cells. **2016**.
8. Wang, Y.; Hamann, T.W. Improved Performance Induced by in-situ Ligand Exchange Reactions of Copper Bipyridyl Redox Couples in Dye-Sensitized Solar Cells. **2018**, 1–14.
9. Furer, S.O.; Milhuisen, R.A.; Kashif, M.K.; Raga, S.R.; Acharya, S.S.; Forsyth, C.; Liu, M.; Frazer, L.; Duffy, N.W.; Ohlin, C.A.; et al. The Performance-Determining Role of Lewis Bases in Dye-Sensitized Solar Cells Employing Copper-Bisphenanthroline Redox Mediators. **2020**, *2002067*, 1–13.